A cost model for ocean iron fertilization as a means of carbon dioxide removal that compares ship- and aerial-based delivery, and estimates verification costs.

David Emerson[1*], Alexander B. Michaud[1], Stephen D. Archer[1], Laura E Sofen[1], Benjamin S. Twining[1]

[1]Bigelow Laboratory for Ocean Sciences, East Boothbay, ME 04544

*Corresponding author

This paper is non-peer reviewed submitted to EarthArXiv; the manuscript is currently under review at Earth's Future.

Key Points:

- Variability in key oceanographic parmeters can impact costs of ocean iron fertilization by 100-fold.
- The model finds aerial-based delivery of iron may reduce costs by 30 – 40% compared to ship-based delivery.
- The cost of verification and enviromental monitoring may increase overall costs of ocean iron fertilization by 3 – 4fold.

Abstract.
This paper presents a cost model for implementing a deployment scale effort for conducting ocean iron fertilization (OIF) for marine-based carbon dioxide removal (CDR). The model incorporates basic oceanographic parameters critical for estimating the effective export of newly fixed CO_2 into biomass that is stimulated by Fe addition to an Fe-limited region of the Southern Ocean. Estimated costs can vary by nearly a 100-fold between best-case and worst-case scenarios with best-case values of \$7/net ton C captured versus worst-case \$1500/net ton C captured, without accounting for verification costs. Primary oceanographic factors that influence cost are the net primary productivity increases achieved via OIF, the amount of carbon exported into the deep ocean, and the amount of CO_2 ventilated back to the atmosphere. The model compares ship-based versus aerial delivery of iron to the ocean, and estimates aerial delivery can be 30 – 40% more cost effective; however, the specific requirements for aerial delivery require additional research and development. The model also estimates costs associated with verification and environmental monitoring of OIF. These costs increase \$/net ton C captured by 3 – 4-fold. Best, intermediate, and worst cases for aerial delivery and ship delivery are \$23, \$83, \$1,735, and \$25, \$94, \$4481, respectively, inclusive of verification costs. The primary goal of this model is to demonstrate the variability in cost of OIF as a CDR method, to better understand where additional research is needed to determine the major factors that may make OIF a tractable, nature-based CDR method.

1. Introduction

The latest IPCC projections for 1.5°C to 2°C of global warming by 2100 are now based on an overshoot in greenhouse gas (GHG) emissions that will require implementation of negative emission technologies (NETs) to actively remove and store excess GHGs to achieve a <2°C trajectory. (H.-O. Pörtner et al., 2022). Estimates for the amount of annual CO_2 removal (CDR) required by 2100 range from 8.5 – 19 Gt/yr (equivalent to 2.3 – 5.2 Gt C/yr) based on one recent analysis (Strefler et al., 2021). NETs fall into two broad categories: 1) novel technical approaches, like direct air capture, or 2) enhancement of natural carbon dioxide removal (CDR) processes. The latter processes may be terrestrial- or marine-based, and generally fall into either enhanced chemical weathering, or promoting photosynthetically-driven CO_2 fixation, coupled to a means for permanent or semi-permanent removal of newly fixed-CO_2 from the atmosphere (F. Wang et al., 2021). Ocean iron fertilization (OIF) is a marine-based NET in this latter class that proposes to add an iron source to parts of the ocean that are iron-limited (GESAMP, 2019). Alleviating this iron limitation results in increased primary production by marine phytoplankton that increases their fixation of CO_2 that is ultimately drawn from the atmosphere. A portion of the biomass is exported to the ocean depths where the newly fixed carbon is removed from the climate system for 10's to 100's to 1000's of years, based on the biomass export depth in the ocean. Since nearly one-third of the global ocean is iron-limited, the potential for OIF for atmospheric CO_2 drawdown is significant, on the order of a gigaton or more per year when integrated over the global ocean (*NAS*, 2022; Williamson et al., 2022)

The recognition of iron's role as an important limiting nutrient and thus controlling factor in rates of CO_2 uptake and fixation in the global ocean is relatively new. It was first proposed in 1980s (Martin & Gordon, 1988; Martin & Fitzwater, 1988). Coincident with the recognition of iron as a limiting nutrient in the modern ocean was paleoclimate analysis indicating that iron supply, primarily as wind-blown aeolian dust delivered from the continents to the open ocean, was one of several factors that controlled atmospheric CO_2 concentrations during the glacial-interglacial periods of the past several hundred thousand years (Lamy et al., 2014; Martin, 1990; Martínez-García et al., 2014; Struve et al., 2022). Combined, these factors led to the hypothesis that active addition of Fe to Fe-limited regions of the ocean, often referred to as high nitrate, low chlorophyll (HNLC), could stimulate enough additional phytoplankton growth that the resultant export of newly fixed CO_2 into the deep ocean could be an effective means of CDR for the mitigation of anthropogenic GHG-induced global warming.

A series of 12 meso-scale Fe additions starting in 1993 (IronEX1) and ending in 2009 (LOHAFEX) were undertaken to first test the idea of Fe as an important limiting nutrient, and secondarily, to understand the effects of Fe fertilized phytoplankton blooms on carbon export. These experiments have been reviewed previously (Boyd et al., 2007; Yoon et al., 2018), and will not be addressed in detail here. Suffice it to say, most Fe additions resulted in substantial phytoplankton blooms whose chlorophyll production could be tracked from space; however, the amount of carbon export to ocean depths was variable, or poorly constrained due to lack of measurements. Nonetheless, these experiments corroborate results from natural Fe fertilization events (Blain et al., 2007; Schine et al., 2021), volcanos (Duggen et al., 2010; Hamme et al., 2010), iceberg melting (Koffman et al., 2021; Schroth et al., 2011), or forest fires, demonstrating that Fe added to HNLC oceanic regions stimulates substantial bloom events and may lead to significant carbon export.

There has been a more than decade long cessation of research into OIF as a NET. In part, this was due to the ambiguous carbon export results from meso-scale Fe addition experiments, and debate over the potential negative impacts of OIF. Early efforts at commercialization of OIF to acquire carbon credits were met with skepticism from the oceanographic community due to concern that the inherent ocean processes involved were not well enough understood to safely commercialize OIF (Strong et al., 2009). An ill-advised attempt to improve fisheries by unlicensed dumping of Fe in the Northeast Pacific in 2012 led to establishment of legal norms through the Law of the Sea that further dampened efforts at developing OIF as a NET (Gambardella, 2019). This controversial background for OIF is, however, set against the accumulating evidence for the negative consequences of climate change on human civilization, the lack of progress in curbing anthropogenic emissions of GHGs, and recognition that NETs, in addition to substantial reductions in GHG emissions, are necessary to maintain global temperature increases at levels not considered catastrophic. It is increasingly important to consider multiple CDR approaches. A recent study from the US National Academy of Science on CDR approaches in the ocean reported that research into OIF is a worthy goal in light of new understanding of the ocean's role in controlling atmospheric CO_2 levels (*NAS*, 2022).

A feasible CDR method must be economically viable in terms of its USD per ton of C removed, and not emit more CO_2 or other GHG equivalents during delivery and monitoring, than will be sequestered due to the OIF treatment (Burns et al., 2017). The goal of this work is to develop a simple cost model for OIF. In addition to being a basic economic analysis, a cost model serves several purposes. It puts a tangible value or cost on uncertainty, and indicates where the costs associated with uncertainty are greatest. This can provide a framework for guiding additional research aimed at constraining this uncertainty. A cost model requires a systematic evaluation of the different logistical processes associated with an approach, and uses a common metric of USD per ton of C sequestered to evaluate these processes. In addition, legal precedence prefers cost-benefit type analysis that puts a dollar value on an 'entity' in terms of creating or amending regulatory laws (Frantzeskaki et al., 2019). This work builds from a similar cost model developed by Harrison (Harrison, 2013) for OIF. The work here presents new information on aerial versus ship delivery; accounts for verification costs and environmental impact assessment, and is updated in terms of our continually improved understanding of the iron cycle in the ocean.

2. Model Development.

2.1 Model Considerations.

Scenario. This cost model presents scenarios for a hypothetical OIF effort in the Southern Ocean aimed at seeding a 200,000 km^2 region (1% of the entire area of the Southern Ocean). The model assumes a square 450 km (240 nautical miles) on a side will be fertilized uniformly, Fig 1. This scale is significantly greater than any previous OIF experiments, and more in line with an actual OIF-based CDR deployment. It's important to point out that research-based applications required to further evaluate the efficacy of OIF will, at least initially, be substantially smaller in size than the scenario proposed here, and may incur significantly higher costs driven by the specific objectives of a given research effort. It is also important to emphasize that this cost model is not a business model, and does not take into account overhead costs, administrative costs, and other business associated costs

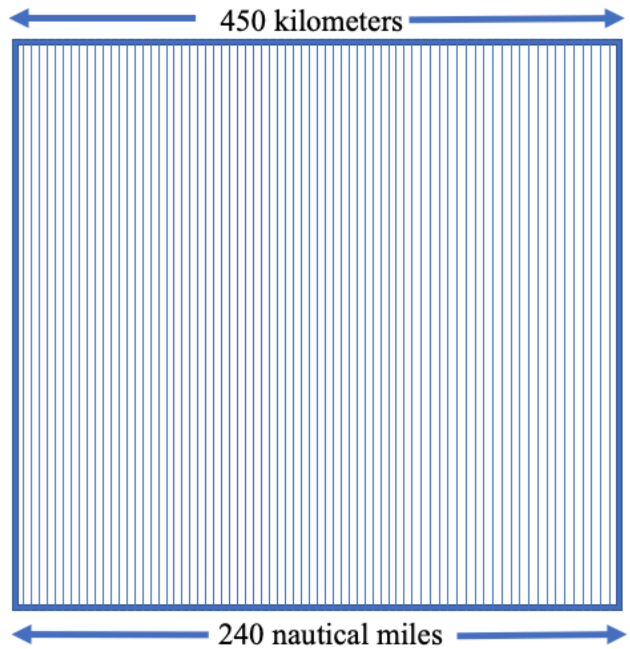

Figure 1. Diagram of deployment scenario for applying iron to a 200,000km^2 area of ocean. This assumes a uniform distribution pattern of 90 swaths with a 5km distance between swaths. For a base model projection of 10d for one OIF application, ship delivery would occur at 15 knots, equivalent to 1.5 swaths/d; aircraft delivery would be 3 swaths/flight with a 4.5h total flight time. The target area is assumed to be 1,500 km from land (nearest port/airport) with a 4d transit time, to and from, for a ship, and 3h transit time, to and from, for a plane.

The oceanographic parameters that contribute to exported carbon (C_{exp}) are summarized as follows: addition of a limiting micro-nutrient, Fe, to an optimal concentration which stimulates photoautotrophy (Fe_{opt}) leading to a net increase in net primary productivity (NPP) that drives uptake of CO_2 to produce new biomass, defined as particulate organic carbon (POC), a proportion of which is exported below the pycnocline that is determined by the mixed layer depth (MLD) of the ocean during a phytoplankton bloom period of finite length. The amount of Fe required is a function of the optimal Fe concentration required to overcome Fe limitation within the MLD of the surface ocean area being fertilized, and the capacity of that Fe source to be utilized by phytoplankton. The following equation summarizes the Fe_{req} in terms of total amount of Fe in ton s.

$$Fe_{req} = ((Fe_{opt} * Fe_{sol}) * MLD) * A_{fert} \qquad (1)$$

In this case Fe_{opt} is the Fe targeted seawater concentration (nmol Fe $\cdot$ L^{-1}) and Fe_{sol} is a unitless solubility fraction that estimates the amount of added Fe that is available for biological uptake. The total amount of C_{exp} is governed by the export efficiency ($C\text{-}Exp_{eff}$) of newly produced biomass or NPP, the total area being fertilized (A_{fert}), as well as the number of OIF applications (App_{num}) during the growing season based on the following equation.

$$C_{exp} = (A_{fert} * NPP_{stim} * C\text{-}Exp_{eff}) * App_{num} \quad (2)$$

These processes underlie the cost model developed here that is based on a simple linear model developed by Harrison (Harrison, 2013).

$$C_{seq} = C_{exp} * [1\text{-}(L_{vent})] \quad (3)$$

$$C_{net} = C_{seq} - (Off_{N2O} + Off_{process} + Off_{verif}) \quad (4)$$

This has two terms: C_{seq} (tons) which is the OIF-stimulated sequestration of C into the ocean taking into account losses in C export (C_{exp}) due to export inefficiencies driven by ventilation (L_{vent}) of CO_2 due to remineralization of POC below the MLD. C_{net} represents the net amount of C (tons) sequestered, accounting for reductions in C_{seq} due to factors that offset C_{net}. These offsets are due to nitrous oxide production (Off_{N2O}; converted to CO_2-equiv) and CO_2-based GHG emissions ($Off_{process}$) resulting from production and delivery of iron for OIF, as well as ship-based verification of carbon export from OIF treatments (Off_{verif}).

To relate C_{net} to an actual cost of OIF in USD per ton C removed ($C), the term Fe_{req} is multiplied by the USD cost of producing and delivering the Fe (Fe_{cost}), plus the USD cost of verifying the carbon export from OIF (Fe_{verif}), to determine USD per ton C that is net sequestered.

$$\$C = (Fe_{req} * (Fe_{cost} + Fe_{verif}))/C_{net} \quad (5)$$

Details for the terms used in the model, including verification requirements, are described below, as well as the additional underlying assumptions in the model that are outlined above. We then use the model to compare ship-based delivery to plane-based delivery of Fe for OIF. The model itself is available as a supplemental table.

3. Description of Model Components. This section covers some of the primary components and related assumptions that go into the model.

3.1Fe Availability, Processing, and Delivery.

<u>3.1.1 Fe solubility.</u> The fraction of Fe that can be readily taken up by phytoplankton and other organisms that is thought to be bioavailable. Bioavailability is a function of the solubility and retention time in the photic zone of the water column of a given Fe source. The solubility is important, since the amount of truly soluble Fe(II) in ocean water is vanishingly small due to thermodynamic and kinetic factors, thus Fe will typically exist in i) a colloidal form of Fe(III); ii) either Fe(II) or Fe(III) that is ligand bound, or iii) as fine particles (e.g. <0.4 μm) of Fe-oxide (Croot & Heller, 2012). These forms are collectively referred to as dissolved iron or dFe. In the case of Fe-oxides, the crystallinity of the oxide will affect its bioavailability, with more crystalline forms like hematite or magnetite being less available than ferrihydrite (Huang et al., 2021). Aeolian dust, a primary source of Fe to the open ocean, generally contains more crystalline, fine particles of hematite with reduced bioavailability (Duce et al., 2009). Sources of Fe used for OIF should maximize bioavailability to maximize phytoplankton uptake efficiency.

The exact uptake mechanism(s) for Fe acquisition, and form of Fe that is most easily acquired, are relatively poorly understood for many pelagic marine phytoplankton.

3.1.2 Fe production and processing. The source of Fe for previous ship-based OIF applications was acidified ferrous sulfate produced by mixing powdered $FeSO_4 \cdot 7H_2O$ with industrial grade HCl, yielding a solution of approximately 30% Fe by weight (300g/kg) (Boyd et al., 2007). The estimated cost for these materials is $700/ton. Pigment grade finely powdered Fe-oxide can be purchased for around $1,000 per ton (https://www.novapolychem.in/hyrox-iron-oxide-pigments.html). Biogenic Fe-oxides have been proposed as another alternative Fe-source (Emerson, 2019); however, these have not been produced at any kind of industrial scale, thus it is difficult to assign a cost. The form of iron used will impact solubility. Iron sources also come with a CO_2 offset due to their production. Commercially available sources of iron are derived from mined iron ores. Estimates for the raw materials extraction of iron ore are 80 kgCO_2e/ton of iron produced, further processing costs are difficult to assess for the types of iron proposed here, but iron agglomeration costs, which is the first processing step in converting iron ore to steel, range from 235 kgCO_2e/ton to 40 kgCO_2e/ton, depending on whether coal or natural gas, respectively, is used for this step (IEA, 2020). Taking a more conservative approach we estimate 305 kgCO_2eq/ton (83 kgC_{eq}/ton) produce for each ton of iron used in an OIF application, as an offset to CO_2 captured. Because it is not well constrained, and is a relatively small number, we have not incorporated this offset in the model.

3.1.3 Fe delivery. For this model we propose two different delivery options for iron to the fertilized area, either ship or plane. Previous mesocosm-based iron additions have been done by ships, using fully research-capable vessels. For the large-scale delivery proposed in this model, we assume that more standard, commercial vessels with significantly lower-cost day rates would be used for open ocean delivery. The model scenario assumes a 10d delivery period over the fertilized area with a swath width of 5 km (Fig 1), projecting a need for 6 ships operating at 15 knots to cover the entire area in 10d, with an additional 6d of transit to and from the site. Fuel consumption costs in CO_{2equiv}, for ships is a known calculable cost, and we assume the Fe-delivery methodology used for earlier mesocosm experiments will be used here (Yoon et al., 2018). This scenario calls for three separate Fe additions during the course of a 120d growing season for phytoplankton in the Southern Ocean.

An alternative to ship-based delivery is aerial application. Aerial application has yet to be tried for OIF. Nonetheless, a major source of iron to the open ocean is air-borne aeolian dust (Hooper et al., 2019; Jickells et al., 2005; Moore & Braucher, 2008; Struve et al., 2022) , thus aerial delivery better mimics natural processes of iron delivery than ship-based methods. Recent well-documented examples of large scale phytoplankton blooms from natural Fe-fertilization events due to volcanos (Duggen et al., 2010; Hamme et al., 2010; Watson, 1997) and wild-fires also resulted in delivery of iron from the atmosphere. To cite one specific example, it is estimated that a large fraction of CO_2 released by the 2019 Australian forest-fires was re-adsorbed into the ocean as a result of phytoplankton bloom, although actual C_{exp} values were difficult to quantify (Tang et al., 2021; Wang et al., 2022). Technologies for the aerial application of agricultural chemicals and fertilizers, or fire-fighting suppressants are well developed, and could be modified for aerial delivery of iron, although this will require at least a moderate amount of R&D to optimize this approach. For the projected OIF scenario, a total of 30 flights at 4h per flight are used to distribute iron over the fertilized area (Fig 1) for each of three total deployments. Aircraft usage costs that could be adapted for OIF are quite well known (Gentile et al., 2022). The primary unknowns are the effectiveness of different forms of iron that could be used, and the specific logistics of dispersion, see Discussion for more considerations around aerial delivery.

3.2 Negative Offsets

3.2.1 Ventilation. Microbially driven remineralization of exported organic matter back to CO_2 may result in ventilation of CO_2 back to the atmosphere, thus reducing permanance of CO_2 initially captured via photosynthesis. While ventilation is dependent on export efficiency of newly produced particulate organic carbon (POC), we include it as a separate term in the model. The major determinant of ventilation is the rate of re-mineralization that occurs below the mixed layer depth. POC is continually re-mineralized to CO_2 as it sinks, and the deeper the depth of remineralization the longer the re-mineralized CO_2 is retained in the ocean interior and out of atmospheric circulation (Kwon et al., 2009) . Martin et al. (Martin, et al., 1987) using a small set of flux measurements established biomineralization rate curves for the open ocean, and estimated globally that 75% of sinking POC was mineralized back to CO_2 by 500m depth, and 90% by 1500m depth. Siegel et al. (Siegel et al., 2021) used a global circulation inverse model (OCIM) to model CO_2-sequestration for the global ocean that compared different CO_2 injection depths to assess how effectively CO_2 was sequestered by the biological pump. This exercise revealed CO_2 injection depth made a large difference in C-sequestration, and estimated that biological pump activity, while inherently leaky, led to approximately 75% of CO_2 ventilated back to the atmosphere in 100 years and 67% in 50 years. This work also showed significant differences based on geographical location in the ocean, with the eastern Pacific and northern Indian Oceans having greater retention, and the Atlantic Ocean having lower retention times. Estimating the amount of CO_2 ventilation is confounded by several factors (Morrison et al., 2022). First, the MLD in the ocean, especially in the higher latitude HNLC regions can increase substantially in the winter. POC that does not sink below the MLD is assumed to be re-mineralized in the same season that it was fixed, i.e., it has no permanence. Second, advective ocean currents can move POC laterally, as well as vertically, and confound estimates of permanence of CO_2 removal, making it difficult to track sequestered CO_2. Third, direct measurements of POC export and re-mineralization in the deep ocean are technically challenging due the high variability of these processes over space and time. Together these factors lead to a substantial amount of uncertainty in how large a factor remineralization and ventilation is in controlling overall export of POC to the ocean interior.

3.2.2 N_2O production. The export of increased amounts of organic matter below the MLD in the ocean due to OIF stimulates enhanced oxic microbial respiration. Due to limited transport of O_2 from the surface ocean across the pycnocline, this increased respiration will result in deoxygenation at depth (Fu & Wang, 2022). As O_2 becomes limiting, nitrate-respiring microbes will increasingly contribute to organic matter consumption resulting in the release of nitrous oxide (N_2O), a GHG with nearly 300 times the potency of CO_2, and an atmospheric residence time of 116(+/-9) years (Tian et al., 2020). Actual measurements of N_2O production in response to OIF field experiments are limited in number, and only followed N_2O production during an OIF experiment. These studies have come to opposite conclusions as to the importance of N_2O

production (Law & Ling, 2001; Walter et al., 2005). Nonetheless, the general principle of N_2O production in response to organic loading in the deep ocean is established (Landolfi et al., 2017), and given the potential for N_2O production to be directly linked to OIF, it is important to include N_2O production as a negative offset in the cost model. We have followed the same rationale as outlined by Harrison (Harrison, 2013) for coupling net C export to N_2O production.

3.3 Verification Costs

3.3.1 Verification Costs. It will be essential to verify the effectiveness of CO_2 removal via OIF, yet verification poses a number of challenges. For the purpose of this modeling exercise, estimated verification costs are integrated into the term $\$C_{net}$ for the monitoring of carbon export. For the model, the costs of verification are based on the day rate for ocean monitoring vessels or aircraft, while others, for example bio-Argo floats represent additional fixed costs. In addition to these actual costs an additional offset (Off_{verif}) for the estimated CO_2 usage required for the ocean-based verification process is included. For the purposes of the model, we assume two ships equipped for verification are deployed for consecutive 70d periods each that will encompass an entire 120d growing season for phytoplankton in the Southern Ocean. These cruises will provide verification data from the three OIF applications via *in-situ* analysis across a set of stations inside the fertilized area, and a smaller set of control sites outside the fertilized area. These ships could also deploy long-term autonomous monitoring floats, as well as autonomous undersea gliders to collect data from a wider area. For the present iteration of the model we are only including ship day rate estimates as the cost parameter for the model

3.3.2 nvironmental Impact Assessment (EIA) Costs. Another important monitoring and cost aspect of the project is to track environmental changes associated with an OIF deployment. Many of the parameters important for environmental impact overlap with verification, for example measurements of changes in nutrients, O_2 concentrations, and pH. Specific EIA-related measurements will focus on more detailed analysis of changes in microbial and phytoplankton community composition, impacts on marine macrobiota, as well as assess toxin-production by phytoplankton blooms.

3.4 Additional oceanographic or biogeochemical factors.

Target Fe concentrations. The concentration of dFe that needs to be added in a specific oceanic region to make it iron replete during a phytoplankton bloom cycle. While phytoplankton taxa vary in the concentration of dFe needed to support maximum growth, a concentration of 0.6 nM is sufficient for most coastal and oceanic species (Sunda, and Huntsman, 1995; Twining, et al., 2021)

Net increase in PP (NPP): The fundamental mechanism for carbon capture via OIF is the increase in the amount of phytoplankton-driven primary production (PP) stimulated by Fe-addition to HNLC regions of the ocean. Estimates of Fe-stimulated NPP are guided by the previous meso-scale Fe-addition experiments (Yoon et al., 2018).

Export efficiency (Exp_{eff}). C export is influenced by a complex set of interactions (Boyd et al., 2019). For simplicity, we refer to as the fractional amount of newly fixed organic carbon exported below the mixed layer depth as particulate organic carbon (POC).

Mixed layer depth (MLD): This is a fixed value, determined by the depth of pycnocline that limits vertical mixing and nutrient supply of surface waters with the deeper ocean waters below. It can be accurately measured, but is variable depending on oceanic region and season.

Bloom length: The number of days during which a bloom is in its active growth phase, with average daily NPP informed by previous OIF experiments.

Length of growing season: The period most amenable to phytoplankton growth, driven by day length, available nutrient concentrations, and temperature. This model assumes that three successive blooms are stimulated during the growing season.

Number of applications: This is a function of Fe bioavailability, especially residence time, related to bloom length and growing season. For the purposes of this modeling exercise, we assume three applications, evenly spaced apart over a presumed phytoplankton growth season and each resulting in 40d bloom. The 40d bloom is composed of a 20d growth phase of the bloom and 20d death phase. The 20d growth phase is what used for quantifying a total amount of new carbon fixed due to OIF.

4. Results.

4.1 Base estimates. Table 1 presents a cost comparison for plane(aerial) versus ship-based delivery of Fe in the OIF scenario outlined above. This scenario assumes an OIF-based stimulation of the primary production rate of 1,000 mgC/m^2/d, and an Exp_{eff} of 10%. Based on three 10d delivery periods during the growing season this yields a total carbon export of 1,200,000 tons (equivalent to 4,400,000 tons of CO_2). Based on this scenario, aerial delivery reduces $\$C_{net}$ by approximately 30% over ship-based delivery (\$4.56/ton C_{exp} vs. \$6.38/ton C_{exp}). In both cases, the fuel usage for delivery, in CO_2equiv is <1% of the C_{exp}.

Table 1. Base cost estimate and comparison for aerial- and ship-based delivery of Fe for an OIF application. This assumes a total of the three individual applications to the same region during one growing season, and is based on intermediate value oceanographic parameters shown in Table 3. These values do not account for offsets or loss, or include verification costs.

Aerial delivery	Parameter	**Ship delivery**	Parameter
Fertilized area	200000 km(2)	Fertilized area	200000 km(2)
C exported	1,200,000 tons	C exported	1,200,000 tons
Total Amount of Fe	1809 tons	Total Amount of Fe	1809 tons
Reagent cost @\$1250/ton	\$2,261,250	Reagent cost @\$750/ton	\$1,356,750
Aircraft & payload	Boeing 373/23.0 tons	Ship requirement	1000 DWT
Operational Cost hourly	\$10,000	Day Rate per ship	\$25,000
Flight duration	4 h	Total cruise duration/ship	60 days

Total flight #/hrs	81/321	Total ship days/6 ships	360
Total Delivery Cost	$3,211,885	Total delivery cost	$5,399,642
Total cost delivery + reagent	$5,473,972	Total cost (delivery + reagent)	$7,661,729
Cost per ton C export	$4.56	Cost per ton C export	$6.38
Fuel usage in CO2 equiv	2,538 tons	Fuel usage in CO2 equiv	8,071 tons
%Offset for aerial delivery	0.22%	%Offset for ship delivery	0.67%

An estimation of the verification and environmental monitoring costs associated with this OIF scenario is shown in Table 2. For the model, we assumed that verification would start within 10d of the end of the first application and continue through the additional two applications and for at least 60d following the final application, including transit times this was two 70d cruises for two ships. This estimate adds an additional $12/ton C_{exp} for verification. This higher cost is driven in part by significantly higher costs for monitoring ships than for delivery ships based on the requirement that verification/monitoring ships will require additional instrumentation and technical personnel to carry out their mission. The other factor that impacts verification costs is the offsets due to fuel usage in CO_{2eqiv}. These offsets become proportionally higher in worst case scenarios where C_{exp} decreases as a result of higher ventilation losses or offsets due to N_2O production, or reduced export efficiency.

Table 2. Estimate of verification/environmental monitoring costs based on base export model not accounting for losses or offsets.

Verification	Parameter
Fertilized area	200000 km(2)
C exported	1,200,000
Ship requirement	Research Vessel
Day Rate per ship	$50,000
No of Ships/cruises	2/2
Ship days/cruise	70
Total ship days	280
Total Cost	$14,000,000
Cost per ton C export	$12.00
Fuel usage in CO2 equiv	14,230
Offset for aerial delivery	1.2%

4.2 Estimates including losses and offsets. This base comparison does not take into account losses in C_{exp} due to ventilation or the offsets due to N_2O production or delivery and verification offsets. To account for these, a series of different scenarios are calculated for best and worst cases for Fe solubility, stimulation of NPP, export efficiency, CO_2 ventilation, and N_2O offset using the values shown in Table 3. The costs for these scenarios in USD/ton C exported for either plane- or ship-based OIF delivery are shown in Table 4, along with intermediate estimates, and best case (lowest cost) and worst case (highest cost) estimates for the different parameters.

The net C exported is shown in Fig 2, and the USD/ton C exported values for the different scenarios are plotted in Fig 3. For each individual comparison the intermediate estimated value for the other values is used for comparison to either the best case or worst case for each individual parameter.

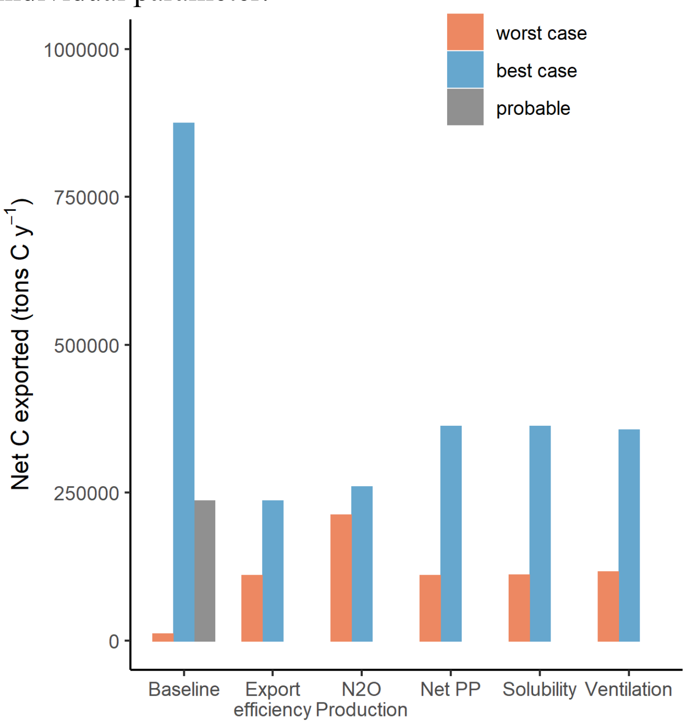

Figure 2. Net carbon exported (C_{net}) under different model scenarios. The model is constructed so that the resulting C_{net} is the same for both ships and planes.

Table 3. Values for major model parameters. Parameters in italics are those that are varied in scenarios between intermediate, best, and worst estimates for values.

Parameter	Units	Intermediate	Best	Worst
Fe solubility	unitless	1.50	1.75	1.10
Stimulation NPP	$mgC/m^2/d$	1000	1500	500
Export Efficiency	$\%C_{org}$ @ 100m	10	15	5
CO_2 Ventilation	$\%CO_2$ re-released	75	65	85
N_2O production	$\%N_2O$ atm release	0.02	0.04	0.06
Fe concentration	nmol/L	0.6		
Mixed Layer Depth	meters	60		
Area Fertilized	km^2	200,000		
Length of Bloom	Days	20		

For ship-based delivery of iron, there is nearly a 170-fold difference in the range of the $C sequestered between the overall best ($9/ton) and worst ($1502/ton) case scenarios, while the best case and intermediate scenarios vary by about a factor of 3. The costs for plane-based delivery of Fe are uniformly less than for ship-based delivery, and there is a nearly 60-fold difference between best ($7/ton) and worst ($415/ton) case scenarios. Variation in ventilation losses due to mineralization of of C_{seq} and differences in the total net primary production each accounted for approximately 3-fold differences between best- and worst-case scenarios, while differences in Fe solubility, C export efficiency, and offsets due to N_2O production accounted for smaller differences using the boundaries that were set in Table 3.

Table 4. Values calculated in USD/ton C ($\$C_{net}$) for different scenarios.

	Plane	Plane and Verification	Ship	Ship and Verification
	USD/ton C exported	**USD/ton C exported**	**USD/ton C exported**	**USD/ton C exported**
Intermediate Estimate	23	83	33	94
Best Case	7	23	9	25
Worst Case	415	1735	1502	4481
Solubility best case	17	56	23	62
Solubility worst case	40	168	68	203
Export efficiency best case	23	83	33	94
Export efficiency worst case	50	178	74	209
Ventilation best case	15	55	22	62
Ventilation worst case	48	169	70	197
N2O Production best case	21	75	30	85
N2O Production worst case	26	92	37	105
Net PP increase best case	15	54	22	61
Net PP decrease worst case	50	178	74	209

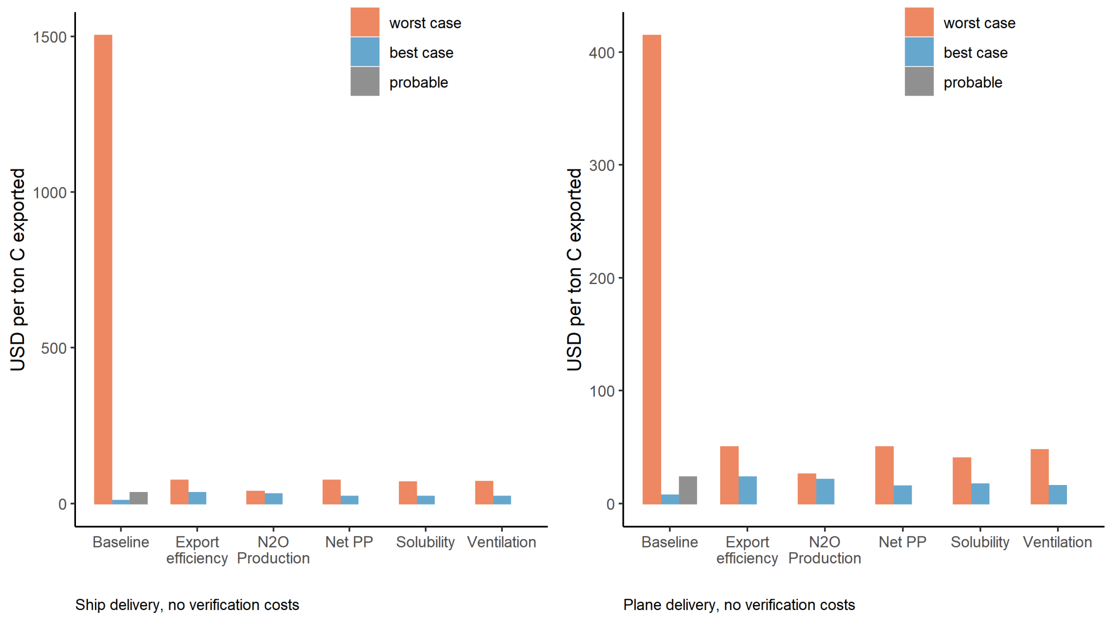

Figure 3. Cost outputs for model under different scenarios. Note the Y-axis is different scales, so plane cost is less than ship-based costs. These cost graphs are for delivery only and do not include verification costs.

5. Discussion.

It is our hope that the results of this cost modeling exercise can help guide research to better understand the major uncertainties that could limit the effectiveness of a large-scale OIF approach to CDR. As expected, the values for USD/ton C sequestered ($C) show a large range (>100-fold) depending upon the values used for the underlying oceanographic parameters. The greatest impacts on cost are estimates for increases in NPP due to OIF, export efficiency, and ventilation. Our mechanistic understanding of both NPP and POC export are relatively well developed (Boyd et al., 2019; Iversen, 2023). NPP can be measured with accuracy using both space-based remote sensing and *in situ* sampling. Export efficiency is more challenging to measure accurately, especially over large spatial scales, but ship-based and autonomous platforms for this purpose are well developed for deployment. By comparison, the magnitude of the ventilation effect on OIF is also large, but substantially more challenging to quantify due to an incomplete understanding of the mechanistic factors that control ventilation (Morrison et al., 2022). This model, thus affirms, that research and testing the ways to quantify both export and especially ventilation are essential to determining the overall efficacy of OIF as a means of CDR.

5.1 Iron Processing and Delivery.

Ship versus Plane. In this cost model, we have purposefully devised a scenario for patch size, and delivery parameters that make cost comparisons between ship and aerially-based delivery as direct as possible. Based on this analysis, the cost per ton C-sequestered ($\$C_{net}$) is approximately 30% less for aircraft compared to ship. The carbon offset for aerial delivery is less than ship-based delivery (0.22% vs 0.67%) for a best estimate, and relatively small in either case. The carbon offset for production of the iron used for OIF is difficult to assess precisely, as discussed above, since it will depend on the form of iron deployed, but due to the relatively small total iron requirement, the processing C offset is likely to be <1% of export.

While the cost model intentionally makes the most direct comparison possible between ship-based and plane-based delivery, in actuality, there are substantial differences in these delivery modes, as well as their associated Fe-seeding strategies. Previous ship-based delivery has used acidified ferrous sulfate injected at the sea surface (Boyd et al., 2007). This delivers a concentrated form of iron effectively as a point source that is diluted and moved initially by vessel propwash, and then by sea-surface currents, wind, and wave action to a wider swath of the ocean. Plane-based delivery would deliver a more dilute iron source over an initially wider swath of ocean. The swath size will depend on aircraft altitude and speed, wind conditions, as well as reagent concentration and matrix. For this scenario, we projected that a dried powdered iron oxide will be used, and delivered from a Boeing 737, or equivalent jet aircraft, flying swath lines at 5 km intervals. It is likely aerial delivery will have more immediate impact on a larger area of the ocean than delivery from a ship. Aerial delivery can also be much faster, depending on the relative number of ships vs planes used, thus the same region could be seeded faster by plane, allowing for faster, or perhaps more synchronized, bloom development. Nonetheless, planes are weight-limited in how much Fe they can deliver per flight, and are more likely to be subject to weather delays than ships.

The potential advantages of aerial delivery need to be balanced by the fact that aerial delivery of iron has not actually been done and will require a research and development phase to determine the most effective dispersal method(s). There is significant technical development around the delivery of agricultural chemicals and fire suppressants via aircraft, , and aircraft-based cloud seeding efforts (Gentile et al., 2022). It is likely some of these technologies could be adapted for aerial delivery of iron; however, these are currently unknowns. The form of iron will also be important. It would be possible to use the same acidified iron solutions as have been used from ships; however, these do incur a significant weight penalty for aircraft, since the solution is only approximately 30% Fe. Alternatively powders of mineral iron oxide could also be used that would have higher Fe yields; however, it would need to be determined if these can be delivered as dried materials, similar to what is done for some fertilizers, or whether a wet slurry would be most effective. Any wetting agent used for aerial delivery will incur an additional weight penalty that increases delivery costs and reduces C_{net}. Other aspects of aerial delivery that need to be considered are photochemical reactions of the iron reagent in the atmosphere that could change its properties, this will be largely dependent on delivery height and residence time in the atmosphere (Ming et al., 2021). Another consideration is transfer of the material across the air-sea interface, which could be impacted by sea surface tension. Despite these caveats, aerial delivery has the potential to not only be less costly than ship-based delivery, but also generate less CO_2 offsets thus increasing C_{net}. Modeling efforts that specifically address critical factors associated with aerial delivery of iron, as well as experimental work on different matrices and photochemical reactions would be useful.

5.2 Verification and Environmental Impact Monitoring.

The substantial monetary cost and CO_2 offset for verification is an important component of this cost model. Based on the model estimates, verification increases total costs for different scenarios by 3- to 4-fold. The verification strategy for this model exercise relies on a combination of ship-based verification measurements extending 60d beyond the end of the last OIF application, as well as the use of autonomous devices. The first verification parameter is confirmation and tracking of bloom dynamics to assess overall increases in primary production. Surface characteristics of bloom dynamics, both intensity and duration, can be monitored by satellite, with ship-based measurements and Bio-Argo floats used to confirm satellite-based measurement and track chlorophyll with depth, as well as determine mixed layer depths. Verification of carbon export needs to take into account a dynamic process that is dependent on sinking depth of POC, remineralization processes, and ocean currents. Specific sets of Bio-Argo floats could be deployed that can monitor aspects of export, changes in pCO_2, O_2 and pH with depth, and other parameters for extended periods (Johnson et al., 2022). Ship-based surveys can deploy sediment traps to measure POC export, track Fe and macro-nutrient concentrations, measure N_2O production, as well as document changes in planktonic communities. A set of aerial overflights of the OIF fertilized patch could measure localized changes in air-sea gas exchange for CO_2, N_2O, methane, and dimethylsulfide (DMS); however, these have not been factored into the cost model. A significant challenge to verification is accounting for longer-term ventilation of CO_2 back to the atmosphere that occurs as a result of POC exported to shallow depths, e.g. <500m, being carried well away from the area being monitored, and then mineralized and re-equilibrated with the atmosphere within months to a few years. Specific to environmental monitoring, the emerging field of environmental DNA (eDNA) will be an invaluable tool (Taberlet et al., 2018), as well as use of autonomous devices that collect genetic and phenotypic data (Ottesen et al., 2011; Olson & Sosik, 2007)) Continued development of autonomous sensors and sensor platforms could significantly reduce the amount of ship-time required for verification and environmental monitoring, which would likely reduce the relative cost.

5.3 Additional implications and impacts.

We have not included the cost of modeling efforts that are tied to OIF applications. It will be essential to have a well constrained coupled physical - biogeochemical – atmospheric model of the chosen fertilized region that is run in real time. In the scenario envisioned, where three successive iron applications are proposed, the model can improve the timing and quantities of Fe used in successive applications, and help guide monitoring efforts, and likely reduce costs. In addition, the model can provide estimates of carbon export and net CO_2 drawdown that can be physically verified. This linkage between model prediction and field measurement will make the model especially useful in refining further OIF applications. Such a model could be especially instructive regarding aerial applications since little is currently known about which key parameters, e.g. delivery altitude, swath width, or speed, are most critical.

One of the most significant negative impacts of large scale and long duration OIF efforts is the potential for nutrient stealing or nutrient robbing. Unused macronutrients in sub-Antarctic and Antarctic waters are exported to lower latitudes via Subantarctic Mode Water (SAMW) and Antarctic Intermediate Water (AAIW) (Sarmiento & Orr, 1991;) Sarmiento et al. 2004; Marinov et al. 2006). Thus, more complete utilization of Southern Ocean nutrients resulting from OIF is likely to subsequently reduce productivity in lower latitudes (particularly equatorial waters). Due to the slow speed of the subsurface currents (decades to traverse from sub-Antarctic to equatorial waters (DeVries, 2014) estimates of this process come from models (e.g., Sarmiento and Orr 1991, Gnanadesikan et al. 2003). (Oschlies et al., 2010) estimate that productivity in waters north of 30˚S is decreased about 10% after implementation of long-term OIF at high latitudes. Tagliabue et al. (2023) also predict a drop in low latitude productivity andsuggest that these OIF-driven reductions in remote productivity may exacerbate productivity declines caused by climate change. The earlier cost model of Harrison (2013) included a nutrient steal parameter that resulted in a 10 – 20% decrease in the effectiveness of OIF; however, due to the projected impacts of nutrient stealing being far removed, in time and space, as well as lack of empirical evidence, we have not included it in this cost model.

This cost model has not taken into account any potential positive GHG offsets, or beneficial aspects, of OIF. One provocative idea is that OIF carried out in the Southern Ocean could help restore the phytoplankton/krill/whale balance that is speculated to have been a significant contributor to marine CDR in this region as little as a century ago (Pearson et al., 2022; Smetacek, 2022.). This balance was upset due to humans harvesting most of the large baleen whales in the Southern Ocean. Contrary to expectations, the reduction in grazing pressure due to reduced whale populations has not resulted in a rebound in krill populations. Recent empirical data on large baleen whale feeding habits in the Southern Ocean, combined with estimates of how much iron these animals may have contributed to the surface ocean through defecation, make a compelling case that this so called 'whale pump' helped maintain greater phytoplankton productivity and krill populations than exist today (Savoca et al., 2021). Determining if it is possible to artificially stimulate the whale pump through specific OIF efforts, and monitoring if there is a direct response of increased whale populations could be an excellent test case for OIF related to both ecosystem restoration, and nature-based CDR.

OIF-induced changes in primary productivity and planktonic community composition, are also likely to alter the extent and composition of trace gases and primary aerosols, including DMS, that exchange between the ocean and atmosphere. This could influence aerosol formation and development, cloud formation and albedo and the oxidative capacity of the atmosphere. Finally, aerial delivery of Fe, depending upon how it is done, could induce photochemical reactions that enhance methane breakdown in the atmosphere (Ming et al., 2021; Oeste et al., 2017). At the present time, we consider any of these potential positive offsets or feedbacks to lack enough empirical evidence for inclusion in a cost model.

An additional limitation of this cost model is that it does not include any expenses related to meeting the regulatory/legal requirements that will need to be addressed to carry out application-based OIF operations (Scott, 2019). The costs necessary to comply with current legal norms associated with OIF will require preparing regulatory documentation, and instituting appropriate oversight for the effort. It is likely these compliance efforts will require a similar timeframe as the fundamental R&D development and planning for an OIF deployment, and will themselves incur a significant cost that is beyond the scope of this model to estimate.

6. Conclusions.

This cost model estimates export costs of carbon in USD per ton of C exported to depths in the ocean where it is stored for at decadal to centennial timescales. Due to the relatively small amounts of Fe that are required to substantially increase net primary production in Fe-limited oceanic regions, costs can be <$10/ton C exported; however, losses due to decreased export efficiency, increased remineralization of exported C, or offsets due to other greenhouse gas production, and other factors can increase costs >100fold. This model directly compares ship-based Fe delivery to aerially-based Fe delivery to the ocean, and estimates aerial delivery can be 30 – 40% less costly. We have also made initial estimates of the cost of verifying C export, and show that ship-centric verification may increase base costs by 3 – 4-fold. The primary aim of this model is to provide direct cost estimates that can aid in development of a research agenda into the efficacy of OIF as a means of CDR. Based on our findings, the magnitude of losses in carbon export efficiency due to ventilation or remineralization of newly fixed biomass, as well as offsets due to N_2O production, are important oceanographic parameters that need to be better understood. Aerial delivery methods for iron maybe beneficial, but due to their novelty for OIF, need specific research and development efforts. Verification methods that primarily utilize autonomous sensors could reduce the need for expensive ship-based methods, but require further development and testing. Finally, oceanographic models localized to the area of OIF application could provide feedback that would maximize effectiveness, and lower the CDR costs of OIF.

Acknowledgements. We thank Dan Whaley for helpful discussions and providing access to a business model developed in the early 2000s for Climos, Inc, that helped assess ship-costs and Fe-reagent costs related to OIF. We thank Dr. Ken Buesseler for comments on an earlier draft of this manuscript. We are grateful for funding from the Grantham Trust for support for this effort.

References:

Blain, S., Quéguiner, B., Armand, L., Belviso, S., Bombled, B., Bopp, L., et al. (2007). Effect of natural iron fertilization on carbon sequestration in the Southern Ocean. *Nature*, *446*(7139), 1070–1074. https://doi.org/10.1038/nature05700

Boyd, P W, Jickells, T., Law, C. S., Blain, S., Boyle, E. A., Buesseler, K. O., et al. (2007). Mesoscale Iron Enrichment Experiments 1993-2005: Synthesis and Future Directions. *Science*, *315*, 612–617. https://doi/10.1126/science.1131669

Boyd, Philip W., Claustre, H., Levy, M., Siegel, D. A., & Weber, T. (2019). Multi-faceted particle pumps drive carbon sequestration in the ocean. *Nature*, *568*, 327–335. https://doi.org/10.1038/s41586-019-1098-2

Burns, W. C. G., Strauss, A. L., Kerstin, G., Oschlies, A., & Proelss, A. (2017). Time to Lift the Research Taboo, *162*, 242–262.

Croot, P. L., & Heller, M. I. (2012). The importance of kinetics and redox in the biogeochemical cycling of iron in the surface ocean. *Frontiers in Microbiology*, *3* 1–15. https://doi.org/10.3389/fmicb.2012.00219

DeVries, T. (2014). The oceanic anthropogenic CO2sink: Storage, air-sea fluxes, and transports over the industrial era. *Global Biogeochemical Cycles*, *28*, 631–647.

Duce, R., Galloway, J., & Liss, P. (2009). The impacts of atmospheric deposition to the ocean on marine ecosystems and climate. *WMO Bulletin*, *58*(58), 61–66.

Duggen, S., Olgun, N., Croot, P., & Hoffmann, L. J. (2010). The role of airborne volcanic ash for the surface ocean biogeochemical iron-cycle: a review. *Biogeosciences*, *7*(3), 827–844.

Emerson, D. (2019). Biogenic iron dust: A novel approach to ocean iron fertilization as a means of large scale removal of carbon dioxide from the atmosphere. *Frontiers in Marine Science*, *6*. https://doi.org/10.3389/fmars.2019.00022

Frantzeskaki, N., McPhearson, T., Collier, M. J., Kendal, D., Bulkeley, H., Dumitru, A., et al. (2019). Nature-based solutions for urban climate change adaptation: Linking science, policy, and practice communities for evidence-based decision-making. *BioScience*, *69*(6), 455–466. https://doi.org/10.1093/biosci/biz042

Fu, W., & Wang, W. (2022). Biogeochemical Equilibrium Responses to Maximal Productivity in High Nutrient Low Chlorophyll Regions. *Journal of Geophysical Research: Biogeosciences*. https://doi.org/10.1029/2021jg006636

Gambardella, S. (2019). The stormy emergence of geoengineering in the international law of the sea. *Carbon and Climate Law Review*, *13*(2), 122–129. https://doi.org/10.21552/cclr/2019/2/7

Gentile, E., Tarantola, F., Lockley, A., Vivian, C., & Caserini, S. (2022). Use of aircraft in ocean alkalinity enhancement. *Science of The Total Environment*, *822*, 153484. https://doi.org/10.1016/j.scitotenv.2022.153484

GESAMP. (2019). High level review of a wide range of proposed marine geoengineering techniques. (Boyd PW and Vivian CMG, eds). *GESAMP Reports and Studies*, *98*(98), 144.

H.-O. Pörtner, D. C., Roberts, M. Tignor, E.S. Poloczanska, K. Mintenbeck, A. Alegría, M. Craig, S. Langsdorf, S. Löschke, V., & Möller, A. Okem, B. R. (eds. . (2022). *No Title Climate Change 2022: Impacts, Adaptation and Vulnerability. Contribution of Working*

Group II to the Sixth Assessment Report of the Intergovernmental Panel on Climate Change. Cambridge, UK. https://doi.org/10.1017/9781009325844

Hamme, R. C., Webley, P. W., Crawford, W. R., Whitney, F. A., DeGrandpre, M. D., Emerson, S. R., et al. (2010). Volcanic ash fuels anomalous plankton bloom in subarctic northeast Pacific. *Geophysical Research Letters*, *37*(19) http://doi.wiley.com/10.1029/2010GL044629

Harrison, D. P. (2013). A method for estimating the cost to sequester carbon dioxide by delivering iron to the ocean. *International Journal of Global Warming*, *5*, 231–254. https://doi.org/10.1504/IJGW.2013.055360

Hooper, J., Mayewski, P., Marx, S., Henson, S., Potocki, M., Sneed, S., et al. (2019). Examining links between dust deposition and phytoplankton response using ice cores. *Aeolian Research*, *36*, 45–60. https://doi.org/10.1016/j.aeolia.2018.11.001

Huang, J., Jones, A., Waite, T. D., Chen, Y., Huang, X., Rosso, K. M., et al. (2021). Fe (II) Redox Chemistry in the Environment. https://doi.org/10.1021/acs.chemrev.0c01286

International Energy Agency (2020). Iron and Steel Technology Roadmap. https://www.iea.org/reports/iron-and-steel-technology-roadmap

Iversen, M. H. (2023). Carbon Export in the Ocean: A Biologist's Perspective. *Annual Review of Marine Science*, *15*, https://doi.org/10.1146/annurev-marine-032122-

Jickells, T. D., An, Z. S., Andersen, K. K., Baker, A. R., Bergametti, C., Brooks, N., et al. (2005). Global iron connections between desert dust, ocean biogeochemistry, and climate. *Science*, *308*, 67–71. https://doi.org/10.1126/science.1105959

Johnson, G. C., Hosoda, S., Jayne, S. R., Oke, P. R., Riser, S. C., Roemmich, D., et al. (2022). Argo-Two Decades: Global Oceanography, Revolutionized. *Annual Review of Marine Science*, *14*, 379–403. https://doi.org/10.1146/annurev-marine-022521-102008

Koffman, B. G., Yoder, M. F., Methven, T., Hanschka, L., Sears, H. B., Saylor, P. L., & Wallace, K. L. (2021). Glacial Dust Surpasses Both Volcanic Ash and Desert Dust in Its Iron Fertilization Potential. *Global Biogeochemical Cycles*, *35*(4). https://doi.org/10.1029/2020GB006821

Kwon, E. Y., Primeau, F., & Sarmiento, J. L. (2009). The impact of remineralization depth on the air-sea carbon balance. *Nature Geoscience*, *2*(9), 630–635. https://doi.org/10.1038/ngeo612

Lamy, F., Gersonde, R., Winckler, G., Esper, O., Jaeschke, A., Kuhn, G., et al. (2014). Increased Dust Deposition in the Pacific Southern Ocean During Glacial Periods. *Science*, *343*, 403–407. https://doi.org/10.1126/science.1245424

Landolfi, A., Somes, C. J., Koeve, W., Zamora, L. M., & Oschlies, A. (2017). Oceanic nitrogen cycling and N_2O flux perturbations in the Anthropocene. *Global Biogeochemical Cycles*. https://doi.org/10.1002/2017GB005633

Law, C. S., & Ling, R. D. (2001). Nitrous oxide flux and response to increased iron availability in the Antarctic Circumpolar Current. *Deep-Sea Research Part II: Topical Studies in Oceanography*, *48*, 2509–2527. https://doi.org/10.1016/S0967-0645(01)00006-6

Martin, J.H., Knauer, G.A., Karl, D.M., Broenkow, W. W. (1987). VERTEX: carbon cycling in the northeast Pacific. *Deep Sea Research*, *34*, 267–285.

Martin, J H. (1990). Glacial-interglacial CO_2 change: the iron hypothesis. *Paleoceanography*, *5*, 1–13.

Martin, J H, & Gordon, R. M. (1988). Northeast Pacific iron distributions in relation to

phytoplankton productivity. *Deep Sea Research Part A Oceanographic 35*(2), 177–196.
Martin, John H, & Fitzwater, S. E. (1988). Iron deficiency limits phytoplankton growth in the north-east Pacific subarctic. *Nature*, *331*, 341–343.
Martínez-García, A., Sigman, D. M., Ren, H., Anderson, R. F., Straub, M., Hodell, D. A., et al. (2014). Iron fertilization of the subantarctic ocean during the last ice age. *Science*, *343*, 1347–1350. https://doi.org/10.1126/science.1246848
Ming, T., Richter, R. de, Dietrich Oeste, F., Tulip, R., & Caillol, S. (2021). A nature-based negative emissions technology able to remove atmospheric methane and other greenhouse gases. *Atmospheric Pollution Research*, *12*(5). https://doi.org/10.1016/j.apr.2021.02.017
Moore, J. K., & Braucher, O. (2008). Sedimentary and mineral dust sources of dissolved iron to the world ocean. *Biogeosciences*, *5*(3), 631–656.
Morrison, A. K., Waugh, D. W., Hogg, A. M. C., Jones, D. C., & Abernathey, R. P. (2022). Ventilation of the Southern Ocean Pycnocline. *Annual Review of Marine Science*, *14*, 405–430. https://doi.org/10.1146/annurev-marine-010419-011012
National Academies of Sciences, Engineering, and Medicine (2022). *A Research Strategy for Ocean-based Carbon Dioxide Removal and Sequestration*. https://doi.org/10.17226/26278
Oeste, F. D., De Richter, R., Ming, T., Caillol, S., Dietrich Oeste, F., De Richter, R., et al. (2017). Climate engineering by mimicking natural dust climate control: The iron salt aerosol method. *Earth System Dynamics*, *8*, 1–54. https://doi.org/10.5194/esd-8-1-2017
Olson, R. J., & Sosik, H. M. (2007). A submersible imaging-in-flow instrument to analyze nano- and microplankton: Imaging FlowCytobot. *Limnology and Oceanography: Methods*, *5*, 195–203. https://doi.org/10.4319/lom.2007.5.195
Oschlies, A., Koeve, W., Rickels, W., & Rehdanz, K. (2010). Side effects and accounting aspects of hypothetical large-scale Southern Ocean iron fertilization. *Biogeosciences*, *7*, 4014–4035. https://doi.org/10.5194/bg-7-4017-2010
Ottesen, E. A., Marin, R., Preston, C. M., Young, C. R., Ryan, J. P., Scholin, C. A., & Delong, E. F. (2011). Metatranscriptomic analysis of autonomously collected and preserved marine bacterioplankton. *The ISME Journal*, *5*, 1881–1895. https://doi.org/10.1038/ismej.2011.70
Pearson, H. C., Savoca, M. S., Costa, D. P., Lomas, M. W., Molina, R., Pershing, A. J., et al. (2022). Whales in the carbon cycle: Can recovery remove carbon dioxide? *Trends in Ecology & Evolution*, 1–12. https://doi.org/10.1016/j.tree.2022.10.012
Sarmiento, J. L., & Orr, J. C. (1991). Three-dimensional simulations of the impact of Southern Ocean nutrient depletion on atmospheric CO2 and ocean chemistry. *Limnology and Oceanography*, *36*(8), 1928–1950. https://doi.org/10.4319/lo.1991.36.8.1928
Savoca, M. S., Czapanskiy, M. F., Kahane-Rapport, S. R., Gough, W. T., Fahlbusch, J. A., Bierlich, K. C., et al. (2021). Baleen whale prey consumption based on high-resolution foraging measurements. *Nature*, *599*(7883), 85–90. https://doi.org/10.1038/s41586-021-03991-5
Schine, C. M. S., Alderkamp, A. C., van Dijken, G., Gerringa, L. J. A., Sergi, S., Laan, P., et al. (2021). Massive Southern Ocean phytoplankton bloom fed by iron of possible hydrothermal origin. *Nature Communications*, *12*(1), 1–11. https://doi.org/10.1038/s41467-021-21339-5
Schroth, A. W., Crusius, J., Chever, F., Bostick, B. C., & Rouxel, O. J. (2011). Glacial influence on the geochemistry of riverine iron fluxes to the Gulf of Alaska and effects of deglaciation. *Geophysical Research Letters*, *38*(16), 1–6. https://doi.org/10.1029/2011GL048367
Scott, K. N. (2019). Mind the gap. In R. C. Beckman, M. Mccreath, J. A. Roach, & Z. Sun (Eds.), *High Seas Governance* (p. 309). Brill Nijhoff, Leiden.

Siegel, D. A., DeVries, T., Doney, S. C., & Bell, T. (2021). Assessing the sequestration time scales of some ocean-based carbon dioxide reduction strategies. *Environmental Research Letters*, *16*(10), 104003. https://doi.org/10.1088/1748-9326/ac0be0

Smetacek, V. (n.d.). News & views A whale of an appetite An algorithm to target COVID testing of travellers.

Strefler, J., Kriegler, E., Bauer, N., Luderer, G., Pietzcker, R. C., Giannousakis, A., & Edenhofer, O. (2021). Alternative carbon price trajectories can avoid excessive carbon removal. *Nature Communications*, *12*(1), 1–8. https://doi.org/10.1038/s41467-021-22211-2

Strong, A., Cullen, J., & Chisholm, S. (2009). Ocean Fertilization: Science, Policy, and Commerce. *Oceanography*, *22*(3), 236–261.

Struve, T., Longman, J., Zander, M., Lamy, F., Winckler, G., & Pahnke, K. (2022). Systematic changes in circumpolar dust transport to the Subantarctic Pacific Ocean over the last two glacial cycles. *Proceedings of the National Academy of Sciences of the United States of America*, *119*(47), 1–10. https://doi.org/10.1073/pnas.2206085119

Sunda, W.G., Huntsman, S. A. (1995). Iron uptake and growth limitation in oceanic and coastal phytoplankton. *Marine Chemistry*, *50*, 189–206.

Taberlet, P., Bonin, A., Zinger, L., & Coissac, E. (2018). *Environmental DNA*. Oxford, UK: Oxford University Press.

Tagliabue, A., Twining, B.S., Barrier, N., Maury, O., Berger, M., Bopp, L. (2023). Ocean iron fertilisation amplifies climate pressures on marine animal biomass. *Global Change Biology*, *In Review*.

Tang, W., Llort, J., Weis, J., Perron, M. M. G., Basart, S., Li, Z., et al. (2021). Widespread phytoplankton blooms triggered by 2019–2020 Australian wildfires. *Nature*, *597*(7876), 370–375. https://doi.org/10.1038/s41586-021-03805-8

Tian, H., Xu, R., Canadell, J. G., Thompson, R. L., Winiwarter, W., Suntharalingam, P., et al. (2020). A comprehensive quantification of global nitrous oxide sources and sinks. *Nature*, *586*(7828), 248–256. https://doi.org/10.1038/s41586-020-2780-0

Twining, B.S., Antipova, O, Chappell, D., Cohen, N R., Jacquot, J., Mann, E.L., Marchetti, A., Ohnemus, D.C., Rauschenberg, S., Tagliabue, A. (2021). Taxonomic and nutrient controls on phytoplankton iron quotas in the ocean. *Limnology and Oceanography Letters*, *6*, 96–106.

Walter, S., Peeken, I., Lochte, K., Webb, A., & Bange, H. W. (2005). Nitrous oxide measurements during EIFEX, the European Iron Fertilization Experiment in the subpolar South Atlantic Ocean. *Geophysical Research Letters*, *32*(23), 1–4. https://doi.org/10.1029/2005GL024619

Wang, F., Harindintwali, J. D., Yuan, Z., Wang, M., Wang, F., Li, S., et al. (2021). Technologies and perspectives for achieving carbon neutrality. *The Innovation*, *2*(4). https://doi.org/10.1016/j.xinn.2021.100180

Wang, Y., Chen, H.-H. H., Tang, R., He, D., Lee, Z., Xue, H., et al. (2022). Australian fire nourishes ocean phytoplankton bloom. *Science of the Total Environment*, *807*, 150775. https://doi.org/10.1016/j.scitotenv.2021.150775

Watson, A. J. (1997). Volvanic iron, CO2, ocean productivity and climate. *Nature*, *385*, 587–588. http://www.plantphysiol.org/content/158/3/1139.full

Williamson, P., Boyd, P. W., Harrison, D. P., Reynard, N., & Mashayek, A. (2022). Chapter 10. Feasibility of Using Biologically-based Processes in the Open Ocean and Coastal Seas for Atmospheric CO2 Removal, (31), 291–350. https://doi.org/10.1039/9781839165245-00291

Yoon, J.-E., Yoo, K.-C., Macdonald, A. M., Yoon, H.-I., Park, K.-T., Yang, E. J., et al. (2018). Reviews and syntheses: Ocean iron fertilization experiments – past, present, and future looking to a future Korean Iron Fertilization Experiment in the Southern Ocean (KIFES) project. *Biogeosciences*, *15*(19), 5847–5889. Retrieved from https://www.biogeosciences.net/15/5847/2018/